

**Anonymous Referee #1** (Review comments in regular; response in bold.)

This paper discusses the aerosol cloud life time effect for the diurnal cycle of Stratocumulus clouds over the ARM SGP site, and comparing the results by a cloud resolving model with those of a GCM. They find that entrainment related evaporation can dominate the autoconversion reduction with increasing aerosol concentration, a mechanism not typically observed in GCMs. In general, I find this paper well written, understandable and novel, so I recommend publication in ACP after some questions are addressed.

Particularly, I am worried about the 50 to 100m horizontal resolution of the CRM, and the 30+ m in the vertical; in most LES intercomparisons of SCu, a much higher resolution is used, particularly to resolve the sharp interface of the SCu top entrainment. Do the authors have a good feel for how well their CRM is converged?

**Answer: We used two horizontal resolutions for the CRM, 50 m and 100 km, not 100m. The response of LWP to increased aerosol number does change signs when we change  $dx=50$  m to  $dx=100$  km but not  $dx=100$  m.**

**To test the convergence of the model, ideally one would increase the resolution of the CRM to see if the results still hold. Due to the limited computational resource we have, we run the cases with a decreased horizontal resolution of 100m. Both  $dx=50$ m cases and  $dx=100$ m cases show the same trend of the LWP, i.e., LWP decreases with increasing aerosol number concentrations. We agree that a resolution with  $dx=50$ m and 30+m in the vertical may be somewhat higher than most LES simulations of SCs and a smaller grid size could be better in capturing the cloud top processes and show some quantitative difference in the LWP. But we expect the trend of LWP to the increased aerosol number will be the same. As the main issue we wish to show is how basic processes left out of GCMs can lead to overestimates of the response of LWP to aerosol particle number, the exact change of LWP is less relevant here. Moreover, we never claimed that we were running the simulation at LES resolutions.**

**The coarse resolution case  $dx=100$ km, was a sensitivity study to mimic what occurs in single column CAM model. We chose this coarse resolution to substantially reduce the vertical movement so that the effect from the microphysics would dominate. By doing this we isolate the microphysics effect from the entrainment effect at the cloud top and demonstrate that using a reduced autoconversion rate in the CRM also increases the LWP when the aerosol number concentrations are increased, which is similar to the response in the GCM.**

The other major question that I have is about the case that they chose. It is a complicated SCu case, with a strong diurnal cycle, and an a-typical qt profile. So why this case, and do you feel it is representative for cloud life time effects across the globe? Perhaps a slightly less generic title would help to lower the expectations here.

**Answer: One of the targeted goals of our funded project was to use the relatively less frequently used IOPs from the SGP site. Thus we chose to use the forcing data derived from the Midlatitude Continental Convective Clouds Experiment (MC3E) which was the most recently conducted experiment near the ARM Southern Great Plains (SGP) site. For this study, May 27th, 2011, was selected because middle and**

**high clouds were absent during a low cloud period observed near noon. We agree that such a case may not be representative enough for SCs across the globe. But the finding (i.e., the absence of cloud-top entrainment effect in GCMs may lead to an overestimated LWP for increased aerosol numbers) should be applicable to SCs with dry air above the cloud top across the globe. To make the title less generic, we change the title from “Why do GCMs overestimate the aerosol cloud lifetime effect? A comparison of CAM5 and a CRM” to “Why do GCMs overestimate the aerosol cloud lifetime effect? A case study comparing CAM5 and a CRM”.**

Other points:

1) It is not very clear from your introduction that you are talking about Stratocumulus, and probably of the kind that barely precipitates. I would make that more clear in the introduction.

**Answer: Done.**

2) How does your work compare with the DYCOMS results, and the papers by Andy Ackerman et al? (e.g., Nature, 2005 and MWR, 2009)

**Answer: Our case is similar to some extent to the DYCOMS-II case in Ackerman et al. (2004) but with even less drizzling. This makes the increased entrainment effect even more dominant than the decreased drizzling effect in our case and explains why we only see decreased LWP with increasing aerosol concentrations. We now mentioned this in the discussion in the revised manuscript.**

3) P2, l 14: Make sure to name your models, and to expand properly

**Answer: Done. We now gave the full name in the abstract.**

4) P3: I am missing a description of your boundary layer scheme here. This is likely a crucial part of information for the CRM entrainment (or lack thereof).

**Answer: Whereas CAM has a shallow convection scheme to parameterize the subgrid transport of heat, moisture, momentum and tracers by asymmetric turbulence within the PBL and a separate moist turbulence scheme for vertical transport by symmetric turbulence (Park and Bretherton 2009), in the CRM, subgrid-scale (turbulent) processes are parameterized using a scheme based on Klemp and Wilhelmson (1978) and Soong and Ogura (1980). The effects of both dry and moist processes on the generation of subgrid-scale kinetic energy have been incorporated. We added this information in the revised manuscript.**

5) Since your resolution is on the lower side for the cloud top: What is your advection scheme in GCE?

**Answer: GCE uses a positive definite advection scheme for scalar variables (Smolarkiewicz and Grabowski 1990).**

6) Also, I have to ask: Is the fact that you are using a bulk micro physics scheme an issue here?

**Answer: We used a 2-moment bulk microphysics scheme which predicts both number and mass mixing ratios of cloud droplets. This scheme has the capability to simulate the**

effect of aerosol indirect effects even though a bin microphysics may follow some of the details more thoroughly.

7) P5, 10: The linear decrease in aerosol means that you have a decreased CCN concentration in the Boundary Layer of about 5%, if my math is correct. Why make that change?

**Answer:**

**Yes, there is a small decrease of CCN with height in the Boundary Layer. This decrease followed the model's default set-up (the aerosol profile is fixed). We agree that the aerosol number should be (well mixed within PBL. But the small decrease assumed in the model should have a very minor impact and will not change the model behavior.**

8) P7, 1: Could you plot the cloud cover as well? The dynamics may very well change as a function of aerosol (or model), for instance moving between cumulus and stratocumulus here.

**Answer: We checked the cloud coverage. The change is negligible when we increase the aerosol number and could not be distinguished any change visually from a height-time plot. All clouds are stratus clouds without any cumulus cloud. In the CAM's microphysics scheme for the rain budget in warm clouds, the source terms of rain include autoconversion and accretion of cloud droplets and the only sink term is the evaporation term of rain. The relatively large decrease of surface precipitation when the aerosol number is increased from 250 to 500  $\text{cm}^{-3}$  is a combination of decreased autoconversion/accretion and increased evaporation of rain. When the aerosol number is increased from 250 to 500  $\text{cm}^{-3}$ , the sum of autoconversion/accretion decreases. Meanwhile since there is less rain falling through the unsaturated sub-cloud layers, the final fraction of rain which can survive evaporation also decreases. The relatively large decrease of surface precipitation is peculiar to the aerosol numbers and environmental conditions. We added a statement to this effect in the manuscript.**

9) P7, 1 18: To mitigate concerns about this particular case, it could be nice to quickly look at a second one as well. But at the very least, a bit more discussion about the dynamics of this case would be appreciated. (e.g., is it decoupled? What is the  $w^2$  profile? How much precipitation do you observe as a function of height).

**Answer: We were not sure whether you were asking about the cases associated with number concentrations or the single day we report in the paper.**

**For number concentration: We checked all cases with different aerosol number concentrations and they have similar structures as showed in Fig. 2b. Fig. 2b actually already presents the results from two cases 250  $\text{cm}^{-3}$  (dash-dotted curves) and 1000  $\text{cm}^{-3}$  (solid curves). But the curves are overlapped. An enlarged portion to distinguish them is presented in Figure S3.**

**Below is a figure showing the profiles of potential temperature, specific humidity, cloud water mixing ratio, rain mixing ratio and  $w^2$ . From the profiles of  $\theta$  and  $q_t$ , we can see the clouds are not decoupled at 14:00 and 15:00. The clouds at 13:00 are a little more**

complicated. The abrupt decrease of  $w^2$  at 1.3 km and the more smooth change of cloud water  $q_c$  and larger  $q_t$ , at this height suggests the clouds above 1.3 km above may not be fully coupled to the sub-cloud layer.

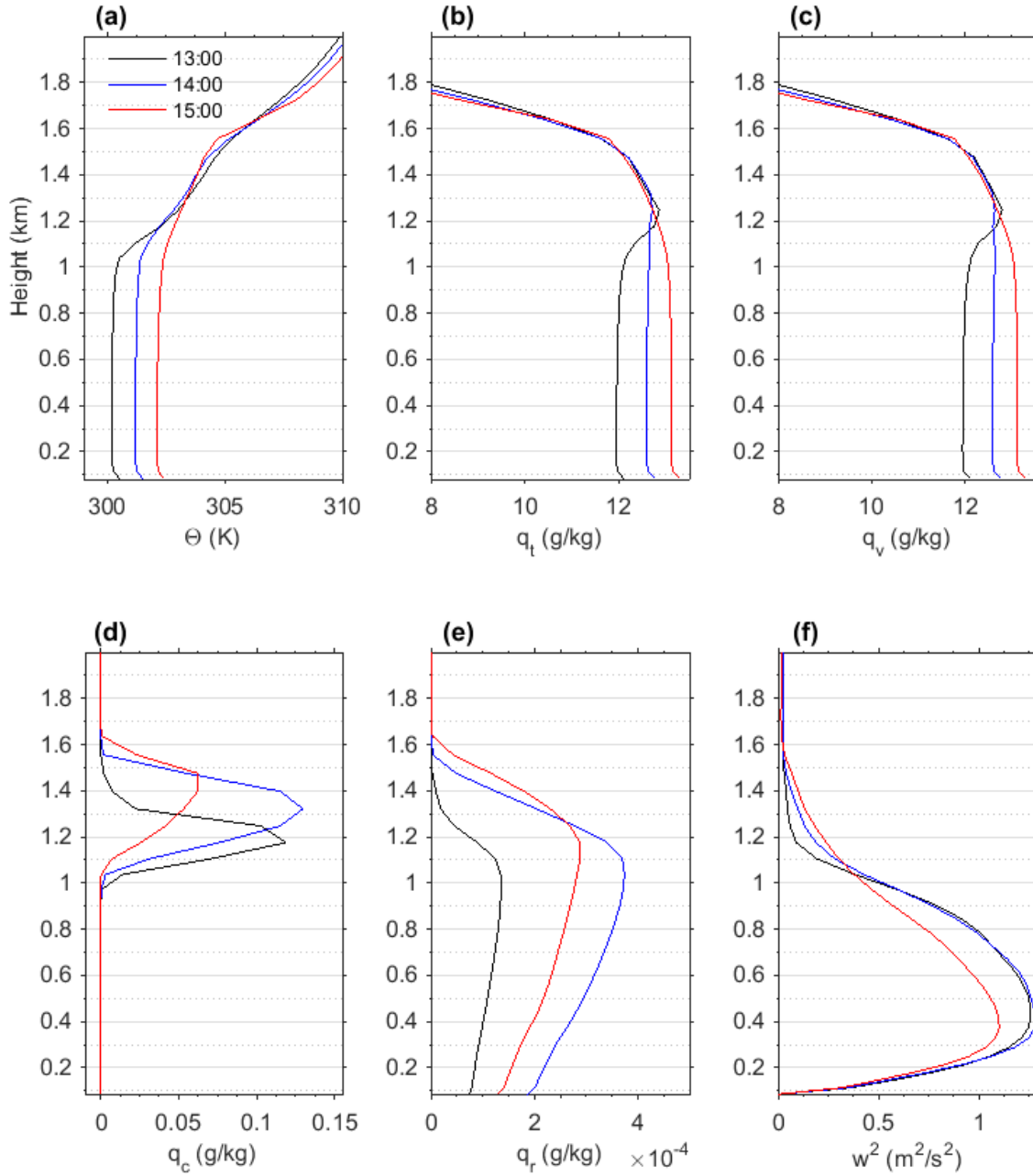


Figure 1 (a) Domain averaged potential temperatures ( $\theta$ ), (b) total water specific humidity ( $q_t$ ), (c) specific humidity ( $q_v$ ), (d) cloud water content ( $q_c$ ), (e) rain mixing ratio ( $q_r$ ) and (f) square of  $w$  at three times (13:00, 14:00 and 15:00) from the GCE case with surface aerosol numbers equal to  $1000 \text{ cm}^{-3}$ .

10) Why do the observations in Figure 1 show no diurnal cycle?

**Answer: The clouds are modulated by advected water vapor and heat fluxes. The fluxes are showed in Fig. S1.**

11) P8, l 22: You state that some differences are likely because of details in the microphysical model. I understand that you cannot get those perfectly identical, but did you do a parameter study to get a feel of this sensitivity?

**Answer: Since aerosol number affects cloud droplet number and thus directly affects the autoconversion rate, we tested the behavior the autoconversion rate to the increasing aerosol number in the two models. As showed in Figure 2 below, autoconversion rates are functions of in-cloud cloud mass mixing ratio and number mixing ratio in both models. Compared to CAM's scheme, autoconversion rates from GCE overall have a smaller dependence on cloud droplet number but larger dependence on cloud mass mixing ratio. We extracted the two pairs of in-cloud droplet number/mass mixing ratios ( [26 cm<sup>-3</sup>, 0.167 g/kg] and [122 cm<sup>-3</sup>, 0.293 g/kg]) from the center layer of clouds at 11:30 hour from the two CAM cases in which the surface aerosol number increasing from 250 cm<sup>-3</sup> to 1000 cm<sup>-3</sup>. The autoconversion rate from the Khairoutdinov and Kogan [2000] scheme used in CAM decreases from 1.86e-9 to 4.67e-10 kg/kg/s. When we applied the GCE's scheme to these two pairs of data the autoconversion rate only decreases from 1.57e-9 to 1.48e-9 kg/kg/s.**

**We added following after the above referenced sentence:**

*“Since the autoconversion rate is directly affected by the aerosol number, we used an offline model to compare the autoconversion rates from the GCE and those from the Khairoutdinov and Kogan [2000] scheme used in CAM. The results are shown in Fig. S4. Compared to CAM's scheme, autoconversion rates from the GCE are less sensitive to the droplet number concentrations when the number concentrations are less than 100 cm<sup>-3</sup> and the cloud mass mixing ratio is above 0.1 g kg<sup>-1</sup>. When the cloud number concentrations are larger than 200 cm<sup>-3</sup>, the autoconversion rates from GCE have a larger dependence on the number concentrations than those from the CAM scheme. However, they have a larger dependence on cloud mass mixing ratio than those from the CAM model. So increasing aerosol number tends to decrease the autoconversion rate more in CAM than in GCE. As an example, we extracted the two pairs of in-cloud droplet number concentrations and mass mixing ratios ( [26 cm<sup>-3</sup>, 0.167 g kg<sup>-1</sup>] and [122 cm<sup>-3</sup>, 0.293 g kg<sup>-1</sup>]) from the center layer of clouds at the 11:30 hour from the two CAM cases in which the surface aerosol number increased from 250 cm<sup>-3</sup> to 1000 cm<sup>-3</sup>. When applying CAM's scheme to these two pairs of data, the autoconversion rate decreases from 1.86 × 10<sup>-9</sup> to 4.67 × 10<sup>-10</sup> kg kg<sup>-1</sup> s<sup>-1</sup>. In GCE's scheme, the autoconversion rate only decreases from 1.57 × 10<sup>-9</sup> to 1.48 × 10<sup>-9</sup> kg kg<sup>-1</sup> s<sup>-1</sup>. ”*

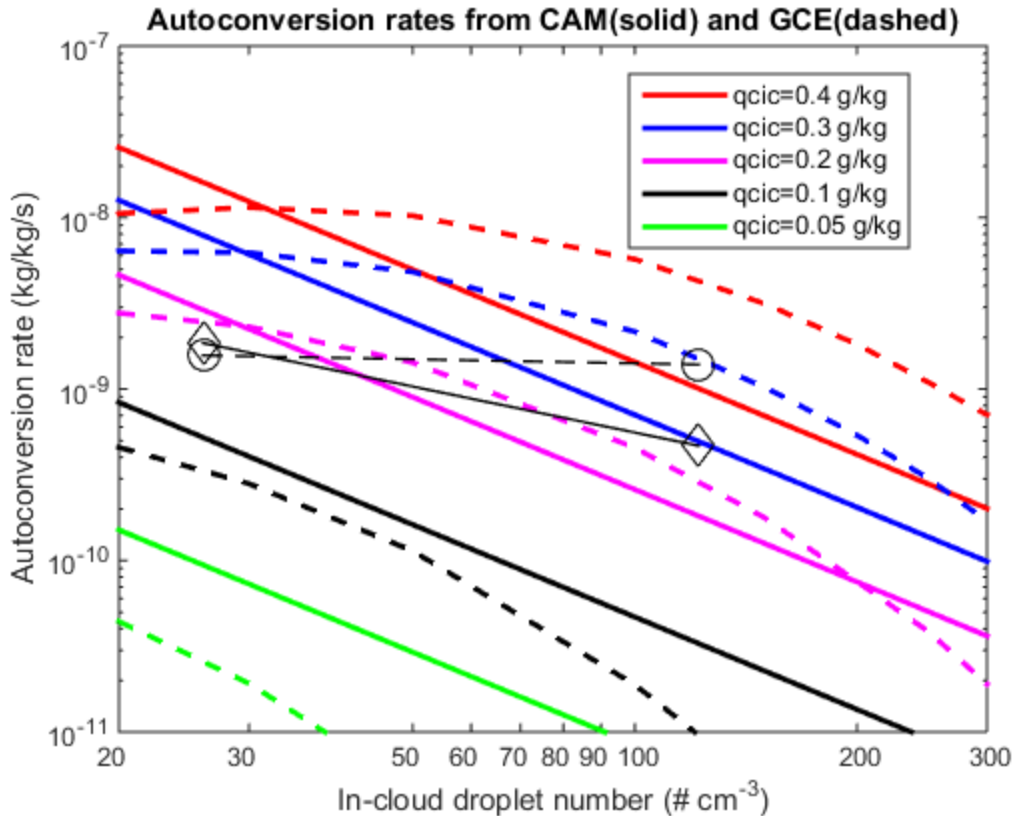


Figure 2. Autoconversion rates from the Khairoutdinov and Kogan [2000] scheme used in CAM (solid curves) and from the stochastic collection equation solutions used in GCE (dashed curves) as functions of in-cloud cloud mass mixing ratio and number mixing ratio. An air density of 1.0 kg/m<sup>3</sup> is used. The two pairs of diamond and circle points are autoconversion rates from the two different schemes (diamond: CAM, circle: GCE) using simulated in-cloud droplet number/mass mixing ratios ([26 cm<sup>-3</sup>, 0.167 g/kg] and [122 cm<sup>-3</sup>, 0.293 g/kg]) which are extracted from the center layer of clouds at the 11:30 hour from the two CAM cases with surface aerosol number equal to 250 cm<sup>-3</sup> and 1000 cm<sup>-3</sup>, respectively.

12) P9, l 21: “..50m to 100km: : :” Should be meter, (I hope)

**Answer: It is 100 km. We choose this coarse resolution on purpose to substantially reduce the vertical movement within the CRM so that the effect from the microphysics would dominate. By doing this we isolated the microphysics effect from the entrainment effect at the cloud top and demonstrated that the reduced autoconversion in the CRM would also increase the LWP when the aerosol number concentrations are increased, which is similar to that in the GCM.**

#### Reference

Klemp, J. B., and R. B. Wilhelmson, 1978: The simulation of three-dimensional convective storm dynamics. *J. Atmos. Sci.*, 35, 1070–1096.

Smolarkiewicz, P. K., and W. W. Grabowski, 1990: The multidimensional positive advection transport algorithm: Nonoscillatory option. *J. Comput. Phys.*, 86, 355–375.

Soong, S.-T., and Y. Ogura, 1980: Response of tradewind cumuli to large-scale processes. *J. Atmos. Sci.*, 37, 2035–2050.

**Referee #2 Ghan** (Review comments in regular; **response in bold.**)

This manuscript presents a clear comparison between two very different models driven by the same boundary conditions but yielding very different results. The analysis clearly reveals the causes of the differences. The work has important implications for global estimates of aerosol effects on clouds.

Lines 29-30. The word “show” is used twice in this sentence. I suggest instead “Observations of ship tracks show that the liquid water path (LWP) in marine boundary-layer clouds can either increase or decrease with increasing aerosol particles : : :”

**Answer: Done.**

Page 3. It’s worth describing the subgrid treatment of cloud microphysics in CAM5: size distribution and subgrid variability.

**Answer: Done. We added following in the revised manuscript:**

*“In-cloud cloud water variability within a GCM grid is considered and represented by an explicit gamma distribution based on observed cloud optical depth variability in marine boundary layer clouds. The subgrid in-cloud water mixing ( $q_c''$ ) follows a gamma distribution  $P(q_c'') = \frac{q_c''^{\nu-1} \alpha^\nu}{\Gamma(\nu)} \exp(-\alpha q_c'')$ , where  $\alpha = 1/q_c'$ ,  $q_c'$  is mean in-cloud mixing ratio and  $\nu$  is chosen to be 1 for simplicity in the model. This subgrid variability function is used to derive factors which can then be applied to calculate microphysical process rates using only the mean in-cloud mixing ratios.”*

Page 4. Does the GCE also use saturation adjustment? How does the dependence of autoconversion on droplet number compare with the KK scheme?

**Answer: The version of GCE used in this study also uses saturation adjustment. Water vapor above saturation is removed at the nucleation step.**

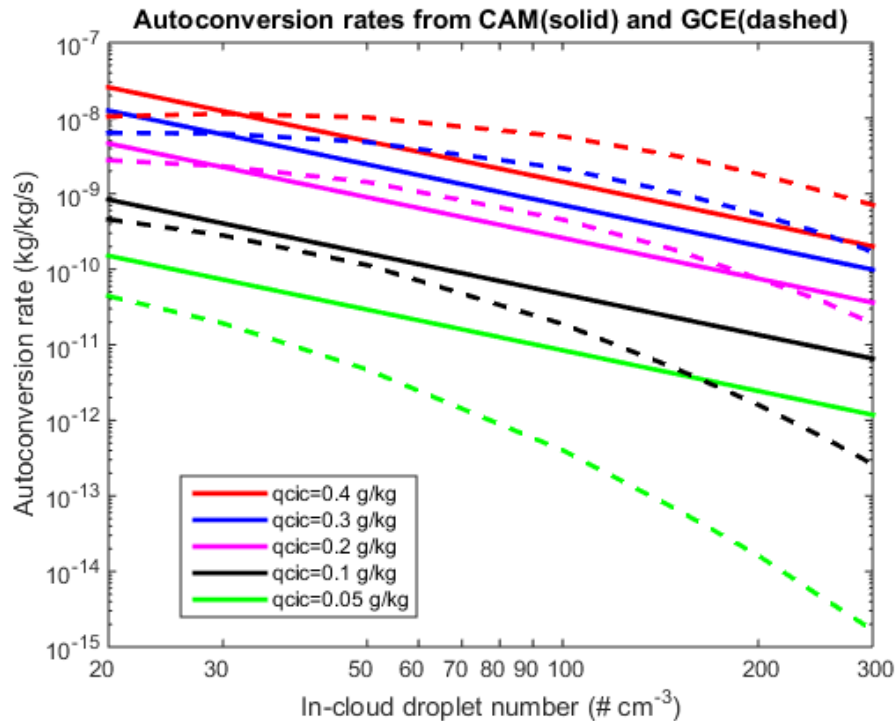




Figure 1. Autoconversion rates from Khairoutdinov and Kogan [2000] scheme used in CAM (solid curves) and stochastic collection equation solutions used in GCE (dashed curves) as a function of in-cloud cloud mass mixing ratio and number mixing ratio. An air density of 1.0 kg/m<sup>3</sup> is used.

**Figure 1 shows autoconversion rates from CAM's Khairoutdinov and Kogan [2000] scheme and the GCE. In both models, autoconversion rates are functions of in-cloud cloud mass mixing ratio ( $q_c$ ) and number concentration ( $N_d$ ). Compared to CAM's scheme, autoconversion rates from GCE are less sensitive to the change of  $N_d$  when  $N_d$  is less than 100 cm<sup>-3</sup> and  $q_c$  is above 0.1 g/kg. When  $N_d$  is larger than 200 cm<sup>-3</sup> and  $q_c$  is above 0.1 g/kg, the autoconversion rates from GCE have a larger dependence on  $N_d$  than CAM's scheme. The autoconversion rates from GCE also show larger dependence on the cloud mass mixing ratio as manifested by the wider vertical range of the curves.**

Page 6, line 19. Start new paragraph here.

**Answer: Done.**

Page 6, line 30. Start new paragraph here.

**Answer: Done.**

Page 7, second paragraph. Please make clear which model is being discussed.

**Answer: Done.**

Page 8, lines 22-24. "This is likely due to the fact that the two models use different cloud droplet activation schemes as well as schemes to parameterize the autoconversion and accretion processes" Please demonstrate this with offline results.

**Answer: Since aerosol number affects cloud droplet number and thus directly affects the autoconversion rate, we tested the response of autoconversion rate to increasing aerosol number in the two models. We extracted the two pairs of in-cloud droplet number/mass mixing ratios ( [26 cm<sup>-3</sup>, 0.167 g/kg] and [122 cm<sup>-3</sup>, 0.293 g/kg]) from the center layer of clouds at the 11:30 hour from the two CAM cases in which the surface aerosol number increased from 250 cm<sup>-3</sup> to 1000 cm<sup>-3</sup>. The autoconversion rate from Khairoutdinov and Kogan [2000] scheme used in CAM decreases from 1.86e-9 to 4.67e-10 kg/kg/s. While applying GCE's scheme to these two pairs of data the autoconversion rate only decreases from 1.57e-9 to 1.48e-9 kg/kg/s. The two pairs of autoconversion rates are added to figure 1 to form a new figure 2 as showed below. We added this figure as Fig.S4 in the supplementary material.**

**We added following after the above referenced sentence:**

*"Since the autoconversion rate is directly affected by the aerosol number, we compared autoconversion rates from GCE and Khairoutdinov and Kogan [2000] scheme used in CAM offline. The results are shown in Fig. S4. Compared to CAM's scheme, autoconversion rates from GCE less sensitive to the number concentrations when the number concentrations are less than 100 cm<sup>-3</sup> and the cloud mass mixing ratio is above 0.1 g kg<sup>-1</sup>. When the cloud number concentrations are larger than 200 cm<sup>-3</sup>, the autoconversion rates from GCE have a larger dependence on the number concentrations than the CAM scheme. However, they have a larger dependence on cloud mass mixing ratio than those from the CAM model. So increasing aerosol number tends to decrease the autoconversion rate more in CAM than in GCE. As an example, we extracted the two pairs of in-cloud droplet number concentrations and mass mixing ratios ( [26 cm<sup>-3</sup>, 0.167 g kg<sup>-1</sup>] and [122 cm<sup>-3</sup>, 0.293 g kg<sup>-1</sup>]) from the center layer of clouds at the 11:30 hour from the two CAM cases in which the surface aerosol number increased from 250 cm<sup>-3</sup> to 1000 cm<sup>-3</sup>. When applying CAM's scheme to these two pairs of data, the autoconversion rate*

decreases from  $1.86 \times 10^{-9}$  to  $4.67 \times 10^{-10} \text{ kg kg}^{-1} \text{ s}^{-1}$ . In GCE's scheme, the autoconversion rate only decreases from  $1.57 \times 10^{-9}$  to  $1.48 \times 10^{-9} \text{ kg kg}^{-1} \text{ s}^{-1}$ . ”

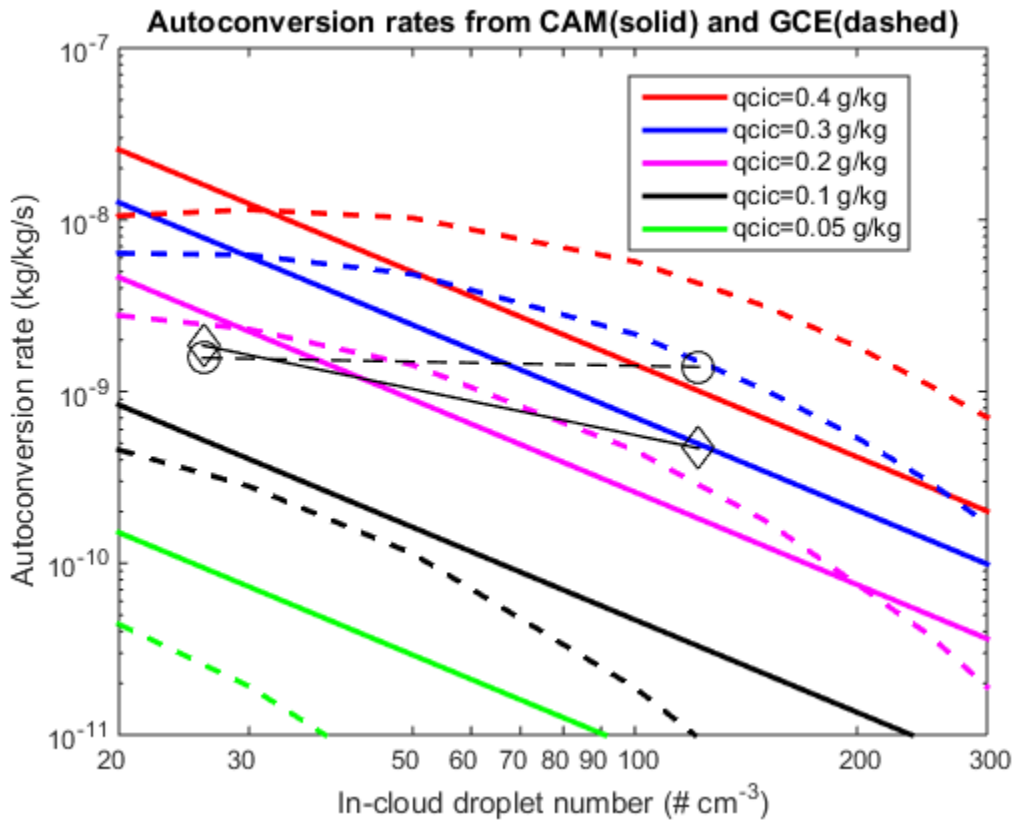


Figure 2. Same as Figure 1 except with 2 added pairs of autoconversion rates from Khairoutdinov and Kogan [2000] scheme used in CAM (diamond) and stochastic collection equation solutions used in GCE (circles). The two pairs of in-cloud droplet number/mass mixing ratio are  $[26 \text{ cm}^{-3}, 0.167 \text{ g/kg}]$  and  $[122 \text{ cm}^{-3}, 0.293 \text{ g/kg}]$  which are extracted from the center layer of clouds at the 11:30 hour from the two CAM cases with surface aerosol number of  $250 \text{ cm}^{-3}$  and  $1000 \text{ cm}^{-3}$  respectively.

Page 9, line 21. Insert “horizontal” before “grid”.

**Answer: Done.**

Page 11, line 3. New paragraph.

**Answer: Done.**

Page 11, lines 10-13. I believe Chris Bretherton tried to implement a treatment of this mechanism in CAM but did not get the desired result. The code for that mechanism might even be in CAM5. I recommend contacting him about that.

**Answer: We contacted with Chris Bretherton and cited the related work.**

1 | **Why do GCMs overestimate the aerosol cloud lifetime effect? A case study comparing**  
2 | **comparison of CAM5 and a CRM**

3 | **Cheng Zhou<sup>1</sup>, Joyce E. Penner<sup>1</sup>**

4 | (1){University of Michigan, Ann Arbor, MI, USA }

5 |  
6 | Corresponding author: C. Zhou (zhouc@umich.edu).  
7 |  
8 |

9 | **Abstract**

10 | Observation-based studies have shown that the aerosol cloud lifetime effect or the  
11 | increase of cloud liquid water path (LWP) with increased aerosol loading may have been  
12 | overestimated in climate models. Here, we simulate shallow warm clouds on 05/27/2011 at  
13 | the Southern Great Plains (SGP) measurement site established by Department of Energy's  
14 | Atmospheric Radiation Measurement (ARM) Program using a single column version of a  
15 | global climate model (Community Atmosphere Model or CAM5.3) and a cloud resolving  
16 | model (CRM). The LWP simulated by CAM increases substantially with aerosol loading  
17 | while that in the CRM does not. The increase of LWP in CAM is caused by a large decrease  
18 | of the autoconversion rate when cloud droplet number increases. In the CRM, the  
19 | autoconversion rate is also reduced, but this is offset or even outweighed by the increased  
20 | evaporation of cloud droplets near cloud top, resulting in an overall decrease in LWP. Our  
21 | results suggest that climate models need to include the dependence of cloud top growth and  
22 | the evaporation/condensation process on cloud droplet number concentrations.  
23 |

24 | **1. Introduction**

25 | Traditionally aerosols have been thought to lengthen cloud lifetime (Albrecht, 1989) by  
26 | increasing droplet number and reducing droplet size thereby delaying and reducing the  
27 | formation of rain in clouds. These longer lived clouds would then increase cloud cover and  
28 | reflect more sunlight. Yet observational evidence for these lifetime effects is limited and  
29 | contradictory (Boucher et al. 2013). Observations of ship tracks show that ~~marine boundary-~~  
30 | ~~layer clouds polluted by aerosol particles show that~~ the liquid water path (LWP) in marine  
31 | boundary-layer clouds can either increase or decrease with increasing aerosol particles  
32 | depending on factors like mesoscale cloud cellular structures, dryness of the free troposphere  
33 | and boundary layer depth (Christensen and Stephens 2011; Chen et al., 2012, 2015). Results

1 from large-eddy simulations (LES) and cloud resolving models (CRM) show the response of  
2 cloud water to aerosols is complicated by competing effects like reduced precipitation  
3 formation efficiency in clouds and enhanced evaporation at cloud top or in the downdraft  
4 regions of cloud edges (Ackerman et al. 2004; Xue and Feingold, 2006; Tao et al., 2012).  
5 Since CRMs and LES models resolve clouds, have more complete physics and depend less  
6 on subgrid parameterizations than general circulations models (GCMs), they are often used  
7 together with field measurements to evaluate and improve parameterizations of clouds and  
8 radiation used in climate models. Several previous studies have compared single column  
9 models, which are essentially an isolated column of a GCM, and cloud resolving models  
10 (Moncreiff et al. 1997; Ghan et al., 2000; Xu et al., 2002; Xie et al., 2002; Xie et al., 2005).  
11 Lee and Penner (2010) extended these types of comparisons to the response of the two  
12 models (CAM and a CRM) to increases in aerosols in thin non-precipitating marine  
13 stratocumulus. Both models found that LWP increased but the effect from increased  
14 condensation dominated in the CRM while the effect from decreased autoconversion  
15 dominated in CAM. Wang et al. (2012) used satellite observations of the precipitation  
16 frequency susceptibility together with model simulations to constrain cloud lifetime effects in  
17 warm marine clouds simulated in GCMs. They show that GCMs tend to overestimate the  
18 precipitation frequency susceptibility of marine clouds. Since the LWP increase as a result of  
19 increased cloud condensation nuclei concentrations is highly correlated with precipitation  
20 frequency susceptibility in climate models, they surmise that the LWP increase is too high  
21 and show that this overestimation could be “fixed” by reducing the dependence of the  
22 autoconversion rate on cloud droplet number in the models.

23 In this study, we simulated continental shallow warm clouds with a very small  
24 precipitation rate ( $< 0.1 \text{ mm day}^{-1}$ ) observed on 05/27/2011 at the Southern Great Plains  
25 (SGP) measurement site established by Department of Energy's Atmospheric Radiation  
26 Measurement (ARM) Program using the single column version of a global climate model  
27 (CAM, version 5.3) and a cloud resolving model and explored plausible causes for the  
28 differences in the response of these two models to increases in aerosols. Here we specifically  
29 identify that the cloud top growth and turbulence mixing parameterizations within CAM  
30 require improvement, rather than only the autoconversion rate. Section 2 describes the  
31 models and set-up. Section 3 presents results followed by conclusions and a discussion in  
32 section 4.

33  
34

1  
2  
3  
4  
5  
6  
7  
8  
9  
10  
11  
12  
13  
14  
15  
16  
17  
18  
19  
20  
21  
22  
23  
24  
25  
26  
27  
28  
29  
30  
31  
32

## 2. Description of models and set-up

We used the Goddard Cumulus Ensemble model (GCE) with recent improvements (Tao et al. 2014) and the single column version of Community Atmosphere Model (CAM, version 5.3) which is the atmospheric component of the Community Earth System Model (CESM, version 1.2.2). Readers are referred to Neale et al. (2012) for more model details of CAM. Here we briefly summarize the two most critical parameterizations for warm stratus clouds in CAM: cloud microphysics and cloud macrophysics. The cloud microphysics (version MG1.5) is a two-moment scheme (Morrison et al. 2005, Morrison and Gettelman 2008) which predicts the number concentrations and mixing ratios of cloud droplets. The source term for the cloud droplets in warm clouds only includes the activation of cloud condensation nuclei while the sink terms include the instantaneous evaporation of falling cloud droplets into the clear portions of grids beneath clouds, autoconversion of cloud droplets to form rain, and accretion of cloud droplets by rain. The first two sink terms (instantaneous evaporation of falling cloud droplets and autoconversion) depend on the aerosol number concentration since the terminal falling speed of cloud droplets is related to cloud droplet size and the autoconversion rate is inversely proportional to cloud droplet number ( $\sim N_c^{-1.79}$  where  $N_c$  is the in-cloud cloud droplet number). The last sink term (accretion) does not depend on the cloud droplet number (Khairoutdinov and Kogan 2000). In-cloud cloud water variability within a GCM grid is based on observed cloud optical depth variability in marine boundary layer clouds. Thus, the sub-grid in-cloud water mixing ( $q_c''$ ) follows a gamma distribution  $P(q_c'') = \frac{q_c''^{\nu-1} \alpha^\nu}{\Gamma(\nu)} \exp(-\alpha q_c'')$ , where  $\alpha = 1/q_c'$ ,  $q_c'$  is mean in-cloud mixing ratio and  $\nu$  is chosen to be 1 for simplicity. This sub-grid variability function is used to derive factors which can then be applied to calculate microphysical process rates using only the mean in-cloud mixing ratios. The conversion of water vapor to cloud condensate is computed by the cloud macrophysics parameterization which also predicts the cloud fraction in each grid as well as the horizontal and vertical overlapping structures of clouds. Following Smith (1990), the liquid fraction of stratus clouds in CAM5 is derived from an assumed triangular distribution of total relative humidity (i.e. the sum of water vapor and liquid cloud water). The net conversion rate of water vapor to stratus condensate is diagnosed using saturation equilibrium conditions: (1) the RH over the water within the liquid stratus is always 100%, and (2) no liquid stratus droplets exist in the clear portion of the grid.

1 The Goddard Cumulus Ensemble model (GCE) is a CRM that has been developed and  
2 improved at the NASA Goddard Space Flight Center (GSFC). Its development and main  
3 features were published in Tao and Simpson (1993) and Tao et al. (2003) and recent  
4 improvements and applications were presented in (Tao et al. 2014). The GCE model used in  
5 the present paper uses the double moment version of the Colorado State University Regional  
6 Atmospheric Modeling System (RAMS) bulk microphysics scheme (Saleeby and Cotton,  
7 2004) which assumes a gamma-shaped particle size distribution for three species of liquid  
8 (small and large cloud droplets and rain). The small cloud droplets range from 2 to 40  
9 microns in diameter, and the large cloud droplets range from 40 to 80 microns. Collection of  
10 cloud droplets is simulated using stochastic collection equation solutions, facilitated by bin-  
11 emulating look-up tables. A positive definite advection scheme is used for scalar variables  
12 (Smolarkiewicz and Grabowski 1990). Sub-grid-scale (turbulent) processes are parameterized  
13 using a scheme based on Klemp and Wilhelmson (1978) and Soong and Ogura (1980). The  
14 effects of both dry and moist processes on the generation of sub-grid-scale kinetic energy  
15 have been incorporated. Readers are referred to Lee et al. (2009) and Tao et al. (2014) for  
16 more detailed descriptions of the model physics.

17 CAM has 30 vertical layers and a variable vertical resolution which depends on the  
18 surface pressure and the vertical temperature profile. In the case studied in this paper the  
19 vertical resolution is roughly 100 meters near the surface and stretches to about 300 m at 2  
20 km decreasing to  $\approx 1$  km at 10 km. The time step is 20 minutes. GCE has 128 grids in the two  
21 horizontal directions and 144 vertical layers. The horizontal resolution is 50 m, so the domain  
22 size is 6.4 km  $\times$  6.4 km. GCE also uses a stretched vertical resolution that varies from about  
23 30 m near the surface to about 90 m at 2 km and further to  $\sim 200$  m at 10 km. The time step of  
24 the GCE model is 1 second. Both models use the same initial conditions (surface  
25 pressure/temperature, vertical temperature/water vapor/wind profiles), boundary conditions  
26 (surface sensible/latent heat fluxes, surface pressure/temperature). Advective tendencies of  
27 temperature and moisture (both vertically and horizontally) are specified based on an  
28 objective variational analysis approach (Xie et al. 2014) fit to the Midlatitude Continental  
29 Convective Clouds Experiment (MC3E) campaign observations which were conducted from  
30 April to June 2011 near the DOE ARM Southern Great Plains (SGP) site. The analyzed  
31 advective tendencies cover the period from April 22<sup>nd</sup> to June 21<sup>th</sup>, 2011. Middle to deep  
32 convective clouds were observed in most cloudy days. For this study, May 27<sup>th</sup>, 2011, was  
33 selected because middle and high clouds were absent during a low cloud period observed  
34 near noon. The vertical wind/temperature/moisture/cloud fraction profiles, surface

1 latent/sensible heat fluxes, and advective tendencies of temperature and moisture are shown  
2 in Fig S1. Low clouds occurred from ~1 km to ~ 2 km near the top of the boundary layer and  
3 were strongly modulated by the advective tendencies of temperature and moisture. Positive  
4 moisture flux and negative temperature flux were observed during the growing stage of the  
5 clouds while negative moisture flux and positive temperature flux were observed during the  
6 decaying stage. Both models are initialized at 00:00 local time and run for 18 hours.

7 To study the effect of aerosols on clouds, we scaled the aerosol vertical profiles in both  
8 models by increasing the surface aerosol number concentrations from  $250 \text{ cm}^{-3}$  to  $4000 \text{ cm}^{-3}$ .  
9 GCE uses a prescribed aerosol profile which decreases linearly from its surface concentration  
10 to  $100 \text{ cm}^{-3}$  at an altitude of 14 km and above. The activation of aerosols to cloud droplets is  
11 based on the grid resolved vertical updraft velocity, temperature, and aerosol number and size  
12 from a look-up table constructed from results of a Lagrangian parcel model (Saleeby and  
13 Cotton, 2004). For CAM, we extracted the averaged aerosol profile in May at this location  
14 from a 5-year run of CAM5 using the MAM3 aerosol module and scaled the aerosol profile  
15 based on the surface aerosol number concentrations (see Fig. S2 for profiles of aerosol  
16 number concentrations used in the two models). The activation of aerosols into cloud droplets  
17 in CAM is diagnosed as a function of the modeled subgrid-scale updraft velocity and aerosol  
18 compositions/sizes/numbers (Abdul-Razzak and Ghan 2000). Even though we set the total  
19 surface aerosol number concentrations the same in the two models, the aerosol composition,  
20 size, and number at cloud level, and the nucleation schemes are inherently different. However,  
21 since this paper focuses on a sensitivity study which is aimed at revealing the different cloud  
22 physical representations in the two models that lead to *opposite* responses of the simulated  
23 LWP to increasing aerosol number concentrations that cover a wide range ( $250 \text{ cm}^{-3}$  to  $4000$   
24  $\text{cm}^{-3}$ ) rather than quantifying the changes of the LWP, these differences are not critical to the  
25 conclusions of the paper. To better isolate differences in the aerosol indirect effect in the two  
26 models, we also turned off the aerosol direct radiative effect.

27

### 28 **3. Results**

29 Figure 1a shows the observed cloud fractions from the early morning to the late afternoon  
30 on May 27<sup>th</sup>, 2011 at the SGP site, while Figures 1b and 1c show the simulated mean cloud  
31 water content from the two models assuming a surface aerosol number concentration of  $500$   
32  $\text{cm}^{-3}$ . Compared to the observations, the simulated clouds from both models begin later in the  
33 day and have a smaller vertical coverage. But the models compare relatively well to each  
34 other which suggests that differences between the models and the observations may largely

1 be caused by the possible errors/uncertainties associated with the derived initial conditions or  
2 advective tendencies. Nevertheless, we can see that the GCE model captures the observed  
3 growth of the clouds with height while CAM does not. A detailed analysis of the GCE (next  
4 paragraph) shows that the clouds could be loosely classified as stratocumulus which occur  
5 near the top of the planetary boundary layer (PBL) and are mainly driven by long wave  
6 radiative cooling offset by short wave radiative heating. This is corroborated by CAM's  
7 result which shows all simulated clouds are stratus clouds and no convective clouds are able  
8 to form above the PBL. The advective tendencies of heat and moisture also strongly modulate  
9 the clouds. For example, the positive moisture tendency before 14:00 hours leads to slightly  
10 larger in-cloud water vapor mixing ratio than that below the clouds (more details will be  
11 presented in the discussion of Figure 2).

12 Figure 1d and 1e show the domain averaged liquid water path (LWP) from the two  
13 models for five different surface aerosol number concentrations (250, 500, 1000, 2000 and  
14 4000  $\text{cm}^{-3}$ ). Both models underestimate the LWP during the day, similar to their  
15 underestimation of cloud cover. GCE shows relatively small changes in the LWP when using  
16 different surface aerosol numbers. The LWP slightly increases with the increasing aerosol  
17 number before ~14:00 but starts to decrease with the increasing aerosol number when the  
18 clouds start to decay after around 14:00. On the other hand, the LWP from CAM increases  
19 substantially and consistently with increasing aerosol number and matches the observed LWP  
20 better when the surface aerosol number is equal to 4000  $\text{cm}^{-3}$ . As noted earlier, due to  
21 uncertainties associated with the derived forcing data as well as uncertainties in the models,  
22 this should not be interpreted as proof that CAM represents the physics better.

23 Figure 1f and 1g show the precipitation rates from the two models. The precipitation rate  
24 from CAM consistently decreases with increasing aerosol number and is nearly suppressed  
25 after 13:00. The change is most prominent when the aerosol number is increased from 250 to  
26 500  $\text{cm}^{-3}$ . This result is due to a combination of decreased autoconversion/accretion and  
27 increased evaporation of rain. When the aerosol number is increased from 250 to 500  $\text{cm}^{-3}$ ,  
28 the sum of autoconversion/accretion decreases. Meanwhile since there is less rain falling  
29 through the unsaturated sub-cloud layers, the final fraction of rain which can survive  
30 evaporation also decreases. The relatively large decrease of surface precipitation is peculiar  
31 to the aerosol numbers and environmental conditions simulated here. The precipitation rates  
32 from GCE are overall very small with maximum values less than 0.08  $\text{mm day}^{-1}$ . The change  
33 in precipitation for GCE with increasing aerosol numbers is a little more complex. During the



1 growing phase of the clouds, as in CAM, the precipitation rate decreases. But during the  
2 decaying phase, the precipitation rate actually increases even though the LWP decreases.

3 Figures 2a-2c show the domain averaged potential temperatures ( $\theta$ ), total water specific  
4 humidity ( $q_t$ ) and cloud water content ( $q_c$ ) at three times (13:00, 14:00 and 15:00) from ~~the~~  
5 two CRM cases with surface aerosol numbers equal to  $250 \text{ cm}^{-3}$  (dash-dotted curves) and  
6  $1000 \text{ cm}^{-3}$  (solid curves), ~~respectively~~.  $q_t$  is the sum of  $q_c$ , rain and water vapor mixing  
7 ratios, which is an invariant within the PBL for stable non-precipitating well-mixed  
8 stratocumulus.  $\theta$  and  $q_t$  from the two cases almost overlap except near the cloud top at 14:00  
9 and 15:00. Fig. 2a shows the growth of the PBL. At 13:00 the clouds do not completely  
10 reside within the PBL as the top of the PBL is at about 1.2 km which is lower than the cloud  
11 top height ( $\sim 1.5$  km) shown in Fig. 2c. Fig. 2b shows that  $q_t$  in the top half of the cloud (from  
12  $\sim 1.2$ - $1.5$  km) is larger than  $q_t$  in the bottom half of clouds (from  $\sim 1$ - $1.2$  km) and  $q_t$  below the  
13 clouds at 13:00. This suggests that the top half of the clouds are not fully coupled with the  
14 surface and the cloud water in the top half of the clouds is strongly affected by the  
15 horizontally advected positive moisture flux. At 14:00 and 15:00, the advected moisture flux  
16 becomes negative and the PBL is high enough that the clouds reside fully within the top of  
17 the PBL and possess the characteristics of well-mixed stratocumulus. The domain averaged  
18 long-wave cooling rate at the cloud top height is about  $2 \text{ K hr}^{-1}$  and is offset by a short-wave  
19 heating of about  $0.5 \text{ K hr}^{-1}$ . Fig. 2c shows that the cloud top is a little higher for the higher  
20 aerosol case, but the maximum values of  $q_c$  are smaller. A closer look at  $\theta$  in Fig. 2a also  
21 shows that the top of the PBL which is near 1.5 km is higher and colder in the higher aerosol  
22 number case. These differences of  $q_c$  and  $\theta$  between the two cases are clearer in an enlarged  
23 portion of Fig 2a and 2b shown in Fig. S3. The potential temperature in the sub-cloud layer at  
24 14:00 and 15:00 is also slightly higher (about  $0.005 \text{ K}$ ) for higher aerosols. Figs. 2d to 2i  
25 show the time-averaged profiles of  $q_c$  and the net result of condensation and evaporation  
26 (Conden-Evap) during two 1-hour intervals (Fig. 2d-f for 13:00 to 14:00 and Fig. 2g-i for  
27 14:00 to 15:00) representing the growing and decaying phases of the cloud, respectively.  
28 Figures 2e and 2h show that a net evaporation occurs just below the cloud base and near the  
29 cloud top. The largest net condensation is located near the cloud base. The most obvious  
30 change between the growing phase and decaying phase of the cloud is the increased  
31 evaporation near the cloud top, especially for the high aerosol number case (see the changes  
32 from blue curve to the red curve at around 1.5 km from Fig. 2e and Fig. 2h). Choosing  
33  $(\text{Conden} - \text{Evap})/q_c$  as a measure of the inverse of the characteristic evaporation time of

1 cloud droplets, Figures 2f and 2i show that it increases substantially from  $300 \text{ hr}^{-1}$  to about  
2  $600 \text{ hr}^{-1}$  (an evaporation time of  $\sim 6$  seconds) near the cloud top for the higher aerosol number  
3 case.

4 Figure 3 shows the LWP and the column integrated LWP source and sink terms from the  
5 low and high aerosol cases ( $250$  and  $1000 \text{ cm}^{-3}$ ). The source term for LWP only includes the  
6 net condensation term (Condens – Evap) while the loss terms include autoconversion and  
7 accretion. Since CAM includes a separate autoconversion and accretion terms while GCE  
8 does not, we combined autoconversion and accretion as one term (Auto+Accre) for easier  
9 comparison. As shown in Fig. 1, when we increase the aerosol numbers from  $250$  to  $1000 \text{ cm}^{-3}$ ,  
10 the LWP increase is relatively small in GCE and substantially larger in CAM. Both models  
11 show decreased Auto+Accre which acts to increase the LWP. This is expected as increased  
12 aerosol numbers increase the cloud droplet number which decreases the autoconversion rate.  
13 But CAM shows much larger changes, especially before 13:00 hours. This is ~~likely~~ due to the  
14 fact that the two models use different cloud droplet activation schemes as well as schemes to  
15 parameterize the autoconversion and accretion processes. Since the autoconversion rate is  
16 directly affected by the aerosol number, we used an offline model to compare the  
17 autoconversion rates from the GCE and those from the Khairoutdinov and Kogan [2000]  
18 scheme used in CAM. The results are shown in Fig. S4. Compared to CAM's scheme,  
19 autoconversion rates from the GCE are less sensitive to the droplet number concentrations  
20 when the number concentrations are less than  $100 \text{ cm}^{-3}$  and the cloud mass mixing ratio is  
21 above  $0.1 \text{ g kg}^{-1}$ . When the cloud number concentrations are larger than  $200 \text{ cm}^{-3}$ , the  
22 autoconversion rates from GCE have a larger dependence on the number concentrations than  
23 those from the CAM scheme. However, they have a larger dependence on cloud mass mixing  
24 ratio than those from the CAM model. So increasing aerosol number tends to decrease the  
25 autoconversion rate more in CAM than in GCE. As an example, we extracted the two pairs of  
26 in-cloud droplet number concentrations and mass mixing ratios ( [ $26 \text{ cm}^{-3}$ ,  $0.167 \text{ g kg}^{-1}$ ] and  
27 [ $122 \text{ cm}^{-3}$ ,  $0.293 \text{ g kg}^{-1}$ ]) from the center layer of clouds at the 11:30 hour from the two CAM  
28 cases in which the surface aerosol number increased from  $250 \text{ cm}^{-3}$  to  $1000 \text{ cm}^{-3}$ . When  
29 applying CAM's scheme to these two pairs of data, the autoconversion rate decreases from  
30  $1.86 \times 10^{-9}$  to  $4.67 \times 10^{-10} \text{ kg kg}^{-1} \text{ s}^{-1}$ . In GCE's scheme, the autoconversion rate only  
31 decreases from  $1.57 \times 10^{-9}$  to  $1.48 \times 10^{-9} \text{ kg kg}^{-1} \text{ s}^{-1}$ . –Moreover, in GCE, the decreased  
32 autoconversion is largely offset or even outweighed by increased evaporation. As shown in  
33 Fig. 2e and 2h the increased evaporation occurs near cloud top. The increased evaporation  
34 near the cloud top and the higher PBL suggests that higher aerosol number concentrations

1 lead to smaller cloud droplet sizes and enhanced evaporation at the cloud top which can then  
2 decrease the temperature slope near the cloud top and promote the sinking of entrained air  
3 into the cloud layer, a point made previously by Bretherton et al. (2007). This evaporation-  
4 entrainment feedback mechanism was also observed in small cumulus clouds (Small et al.  
5 2009). Before ~14:00, the effect from the decreased autoconversion rates outweighs the  
6 effect from increased evaporation so that the LWP shows a slight increase. But as the cloud  
7 starts to decay after ~14:00, the PBL keeps growing and the enhanced  
8 evaporation/entrainment rates accelerate the decaying process. Thus the LWP decreases  
9 faster and eventually a smaller LWP results over the decaying period for the high aerosol  
10 case. In the CAM model, the change of the net condensation term (Condens – Evap) is smaller  
11 than that in the CRM model. Since the simulated cloud top remains unchanged between  
12 12:00 and 15:00 hours, the drying effect seen in the CRM due to enhanced entrainment of  
13 overlying dry air is not present. This is likely due to the fact that the moist turbulence scheme  
14 in CAM does not depend on the cloud droplet number/size and the condensation and  
15 evaporation in the CAM’s microphysics scheme is not linked to the cloud droplet number or  
16 size. Even though the instantaneous evaporation of falling cloud droplets into the clear  
17 portions of grids beneath clouds in the microphysics scheme is related to the cloud droplet  
18 number, it is about one order of magnitude smaller than the net condensation term in the  
19 microphysics scheme. Consequently the net condensation and evaporation is less sensitive to  
20 the change in aerosol number and the effect from the decreased autoconversion rate  
21 dominates the condensate loss, leading to an increase of the LWP.

22 To confirm that the effect from enhanced entrainment at the cloud top is the critical  
23 reason for the reduced LWP change in GCE, we ran a sensitivity test to reduce the cloud top  
24 mixing by increasing the horizontal grid spacing from 50 m to 100 km. With this larger grid  
25 spacing, we greatly reduced the overshooting at the cloud top by reducing the maximum  
26 vertical speed in the updrafts from meters per second to a few centimeters per second. As a  
27 result, the enhanced entrainment effect was reduced and the microphysical effect from the  
28 reduced autoconversion rate dominated. Figure 4 shows that the LWP from GCE decreases  
29 by about 5% for the dx=50 m case while it increases by about 12% for the dx=100 km case  
30 when the surface aerosol number is increased from  $250 \text{ cm}^{-3}$  to  $4000 \text{ cm}^{-3}$ . We also ran two  
31 more tests to explore whether the LWP sensitivity in CAM could match that in the GCE. In  
32 the default set-up of CAM, the autoconversion rate is inversely proportional to cloud droplet  
33 number ( $\sim N_c^{-1.79}$  where  $N_c$  is the in-cloud cloud droplet number). We ran two cases, auto06

1 and auto00, each with a reduced dependence of the autoconversion rate on the cloud droplet  
2 number. In case auto06, the autoconversion rate is proportional to  $N_c^{-0.60}$  and in case auto00,  
3 the autoconversion rate does not depend on the cloud droplet number. The autoconversion  
4 rate is scaled in both cases to produce the same rate as that from the default case at a droplet  
5 number concentration of  $100 \text{ cm}^{-3}$ . As shown in Fig. 4, the LWP from the default case is  
6 more than doubled when the surface aerosol number is increased from  $250 \text{ cm}^{-3}$  to  $4000 \text{ cm}^{-3}$   
7 while the LWP from auto06 only increases by ~50% and the LWP from case auto00 remains  
8 almost unchanged. These results suggest that the dependence of the autoconversion rate on  
9 the cloud droplet number can play a determining role on the simulated LWP consistent with  
10 the findings of precipitation frequency susceptibility in Wang et al. (2012). However, this  
11 adjustment is unable to simulate decreases in LWP seen in the GCE model.

12

#### 13 **4. Conclusion and Discussion**

14 We simulated shallow warm clouds on May 27<sup>th</sup>, 2011 at the DOE ARM SGP site with a  
15 cloud resolving model (Goddard Cumulus Ensemble model) and a single column model  
16 (CAM) using the same initial/boundary conditions and advected moisture/heat tendencies  
17 derived from the MC3E campaign data. The liquid water path (LWP) simulated by CAM  
18 shows a large dependence on the aerosol loading and is more than doubled when the surface  
19 aerosol number is increased from  $250 \text{ cm}^{-3}$  to  $4000 \text{ cm}^{-3}$  while the LWP simulated by the  
20 CRM decreases by ~5%. The high sensitivity of LWP on aerosol loading in CAM can be  
21 reduced by reducing the dependence of the autoconversion rate on the cloud droplet number  
22 concentration, but is unable to reproduce the decrease in LWP seen in the CRM. Whereas  
23 Wang et al. (2012) concluded that this term in GCM models can be tuned to fit observations  
24 of the precipitation frequency susceptibility, we find that the poor representation of  
25 entrainment and droplet evaporation in CAM model may be the fundamental cause of  
26 differences with the more complete CRM. While in the CRM a reduced autoconversion rate  
27 is also observed with increased aerosol loading, it is offset or even outweighed by the  
28 increased evaporation of cloud droplets near the cloud top. The increased evaporation cools  
29 the cloud top, reduces the temperature lapse rate and thus increases the entrainment of drier  
30 air above the cloud top and accelerates the decaying process of the clouds. Reduced LWP  
31 through enhanced entrainment with increased aerosol number has also been reported in  
32 previous literature using large eddy simulations (e.g., [Ackerman et al. 2004](#), Bretherton et al.  
33 [2007](#), Seifert et al. 2015). To some extent our case is similar to the DYCOM-II case studied

1 in Ackerman et al. (2004) with low humidity above the cloud top. Our case has even less  
2 drizzling and this makes the increased entrainment effect even more dominant than the  
3 decreased drizzling effect which explains why we only see decreased LWP with increasing  
4 aerosol concentrations.

5 One unique aspect of the present paper is that the response of the LWP over the lifetime  
6 of the cloud is negative in the CRM while it is positive in the CAM model for the same  
7 forcing conditions. One critical deficiency of CAM for this case is that the effect from  
8 increased mixing of drier air from above the cloud layer through enhanced entrainment  
9 caused by increased aerosol numbers is missing. First, CAM is not able to simulate the  
10 growth of the cloud top due to its coarse vertical resolution. However, even if the CAM  
11 vertical resolution were high enough to capture the growth of the cloud top, since the moist  
12 turbulence scheme and the evaporation of cloud condensate in the cloud macrophysics  
13 parameterization at the cloud top are not related to the cloud droplet number, aerosol number  
14 will not have a direct impact on the cloud top mixing or the LWP. Some effort has been made  
15 to address this issue in CAM. Jones (2013) implemented a droplet sedimentation-entrainment  
16 feedback scheme in CAM. Yet a mixture of the cloud macrophysics and the MG  
17 microphysics still prevent clouds from responding to droplet number changes by thinning or  
18 thickening as demonstrated by other LES simulations.

19 Our CRM model results also demonstrate that the relative importance of the decreased  
20 autoconversion rate effect and the enhanced entrainment effect from increased aerosol  
21 numbers can change based on environmental conditions as manifested in different stages  
22 during the cloud lifecycle. Thus, one may need to distinguish the cloud stage when studying  
23 the aerosol lifetime effect either with a model or from observations.

## 24

## 25 **5. Acknowledgements**

26 This work was supported by the DOE under grant #DOE DE-SC0008486. We thank  
27 Derek Posselt and S.-S. Lee for helpful discussions and setting up the GCE model. We also  
28 thank Shaocheng Xie for providing the ARM forcing data. We acknowledge high-  
29 performance computing support from National Energy Research Scientific Computing Center  
30 (NERSC).

## 31

## 32 **References**

33 Abdul-Razzak, H. and Ghan, S.: A parameterisation of aerosol activation 2. Multiple aerosol  
34 types, J. Geophys. Res., 105, 6837–6844, 2000.

1 [Ackerman, A. S., Kirkpatrick, M. P., Stevens, D. E., and Toon, O. B.: The impact of humidity](#)  
2 [above stratiform clouds on indirect aerosol climate forcing, \*Nature\*, 432, 1014–](#)  
3 [1017, 2004.](#)

4 Boucher, O., et al.: Clouds and aerosols, in *Climate Change 2013: The Physical Science*  
5 *Basis. Contribution of Working Group I to the Fifth Assessment Report of the*  
6 *Intergovernmental Panel on Climate Change*, edited by T. Stocker, et al., Cambridge  
7 Univ. Press, Cambridge, U. K., 2013.

8 Bretherton, C. S., Blossey, P.N. and Uchida J.: Cloud droplet sedimentation, entrainment  
9 efficiency, and subtropical stratocumulus albedo, *Geophys. Res. Lett.*, 34, L03813,  
10 doi:10.1029/2006GL027648, 2007.

11 Chen, Y.-C., Christensen, M. W., Diner, D. J. and Garay, M. J.: Aerosol-cloudinteractions in  
12 ship tracks using TerraMODIS/MISR, *J. Geophys. Res. Atmos.*, 120,2819–2833,  
13 doi:10.1002/2014JD022736, 2015.

14 Chen, Y.-C., Christensen, M. W., Xue, L., Sorooshian, A., Stephens, G. L., Rasmussen, R.  
15 M. and Seinfeld, J. H.: Occurrence of lower cloud albedo in ship tracks, *Atmos. Chem.*  
16 *Phys.*, 12, 8223–8235, 2012.

17 Christensen, M. W. and Stephens, G. L.: Microphysical and macrophysical responses of  
18 marine stratocumuluspolluted by underlying ships: Evidence of cloud deepening, *J.*  
19 *Geophys. Res.*, 116, D03201, doi:10.1029/2010JD014638, 2011.

20 Ghan, S., Randall, D., Xu, K.-M., Cederwall, R., Cripe, D., Hack, J., Iacobellis, S., Klein, S.,  
21 Krueger, S., Lohmann, U., Pedretti, J., Robock, A., Rotstayn, L., Somerville, R.,  
22 Stenchikov, G., Sud, Y., Walker, G., Xie, S., Yio, J., and Zhang, M.: A comparison of  
23 single column model simulations of summertime midlatitude continental convection, *J.*  
24 *Geophys. Res.*, 105, 2091–2124, 2000

25 [Jones, C.: Single-column and mixed-layer model analysis of subtropical stratocumulus](#)  
26 [response mechanisms relevant to climate change, Ph.D. thesis, University of](#)  
27 [Washington, 2013.](#)

28 Khairoutdinov, M. F. and Y. Kogan, A new cloud physics parameterization in a large-eddy  
29 simulation model of marine stratocumulus, *Mon. Weather Rev.*, 128, 229–243, 2000.

30 [Klemp, J. B., and Wilhelmson, R. B.: The simulation of three-dimensional convective storm](#)  
31 [dynamics. \*J. Atmos. Sci.\*,35, 1070–1096,1978.](#)

32 Lee, S. S. and Penner, J. E.: Comparison of a global-climate model to a cloud-system  
33 resolving model for the long-term response of thin stratocumulus clouds to preindustrial

1 and present-day aerosol conditions, *Atmos. Chem. Phys.*, 10, 6371-6389,  
2 doi:10.5194/acp-10-6371-2010, 2010.

3 Lee, S. S., Penner, J. E. and Saleeby, S. M.: Aerosol effects on liquid-water path of thin  
4 stratocumulus clouds, *J. Geophys. Res.*, 114, D07204, doi:10.1029/2008JD010513,  
5 2009.

6 Moncrieff, M. W., Krueger, S. K., Gregory, D., Redelsperger, J.-L. and Tao, W.-K.: GEWEX  
7 Cloud System Study (GCSS) Working Group 4: Precipitating convective systems, *Bull.*  
8 *Am. Meteorol. Soc.*, 78, 831–845, 1997.

9 Morrison, H., and Gettelman, A.: A new two-moment bulk stratiform cloud microphysics  
10 scheme in the NCAR Community Atmosphere Model (CAM3), Part I: Description and  
11 numerical tests, *J. Clim.*, 21 (15), 3642–3659, 2008.

12 Morrison, H., Curry, J. A. and Khvorostyanov, V. I.: A new double-moment microphysics  
13 parameterization for application in cloud and climate models. part i: Description, *J.*  
14 *Atmos. Sci.*, 62, 1665–1677, 2005.

15 Saleeby S. M. and Cotton, W. R.: A large droplet mode and prognostic number concentration  
16 of cloud droplets in the Colorado State University Regional Atmospheric Modeling  
17 System (RAMS). Part I: Module descriptions and supercell test simulations. *J. Appl.*  
18 *Meteor.*, 43, 182–195, 2004.

19 Seifert, A., Heus, T., Pincus, R., and Stevens, B.: Large-eddy simulation of the transient and  
20 near-equilibrium behavior of precipitating shallow convection, *J. Adv. Model. Earth*  
21 *Syst.*, 7, 1918–1937, doi:10.1002/2015MS000489, 2015.

22 Small, J. D., Chuang, P. Y., Feingold, G. and Jiang, H.: Can aerosol decrease cloud lifetime?,  
23 *Geophys. Res. Lett.*, 36, L16806, doi:10.1029/2009GL038888, 2009.

24 Smith, R. N. B.: A scheme for predicting layer clouds and their water content in a general  
25 circulation model, *Q. J. R. Meteorol. Soc.*, 116, 435–460, 1990.

26 [Smolarkiewicz, P. K., and Grabowski, W. W.: The multidimensional positive advection](#)  
27 [transport algorithm: Nonoscillatory option. \*J. Comput. Phys.\*, 86, 355–375, 1990.](#)

28 [Soong, S.-T., and Ogura, Y.: Response of tradewind cumuli to large-scale processes. \*J.\*](#)  
29 [\*Atmos. Sci.\*, 37, 2035–2050, 1980.](#)

30 Tao, W.-K.: Goddard Cumulus Ensemble (GCE) model: application for understanding  
31 precipitation processes. AMS Meteorological Monographs— Cloud Systems,  
32 Hurricanes and TRMM 107–138, 2003.

33 Tao, W.-K., Lang, S., Zeng, X.P., Li, X.W., Matsui, T., Mohr, K., Posselt, D., Chern, J.,  
34 Peters-Lidard, C., Norris, P.M., Kang, I.S., Choi, I., Hou, A., Lau, K.-M. and Yang, Y.-

1 M.: The Goddard Cumulus Ensemble model (GCE): Improvements and applications for  
2 studying precipitation processes, *Atmos. Res.*, 143, 392–424, 2014.

3 Tao, W.-K. and Simpson, J.: The Goddard Cumulus Ensemble Model. Part I: model  
4 description. *Terr. Atmos. Ocean. Sci.* 4, 35–72, 1993.

5 Wang, M., Ghan, S., Liu, X., L'Ecuyer, T. S., Zhang, K., Morrison, H., Ovchinnikov, M.,  
6 Easter, R., Marchand, R., Chand, D., Qian, Y., Penner, J.E.: Constraining cloud lifetime  
7 effects of aerosols using A-Train satellite observations, *Geophys. Res. Lett.*, 39, L15709,  
8 doi:10.1029/2012GL052204, 2012.

9 Xie, S, Xu, K.-M., Cederwall, R. T., Bechtold, P., Genio, A. D. D., Klein, S. A., Cripe, D. G.,  
10 Ghan, S. J., Gregory, D., Iacobellis, S. F., Krueger, S. K., Lohmann, U., Petch, J. C.,  
11 Randall, D. A., et al.: Intercomparison and evaluation of cumulus parametrizations  
12 under summertime midlatitude continental conditions, *Q. J. Roy. Meteor. Soc.*, 128,  
13 1095–1135, 2002.

14 Xie, S., Zhang, M., Branson, M., et al.: Simulations of midlatitude frontal clouds by single-  
15 column and cloud-resolving models during the Atmospheric Radiation Measurement  
16 March 2000 cloud intensive operational period, *J. Geophys. Res.*, 110, D15S03,  
17 doi:10.1029/2004JD005119, 2005.

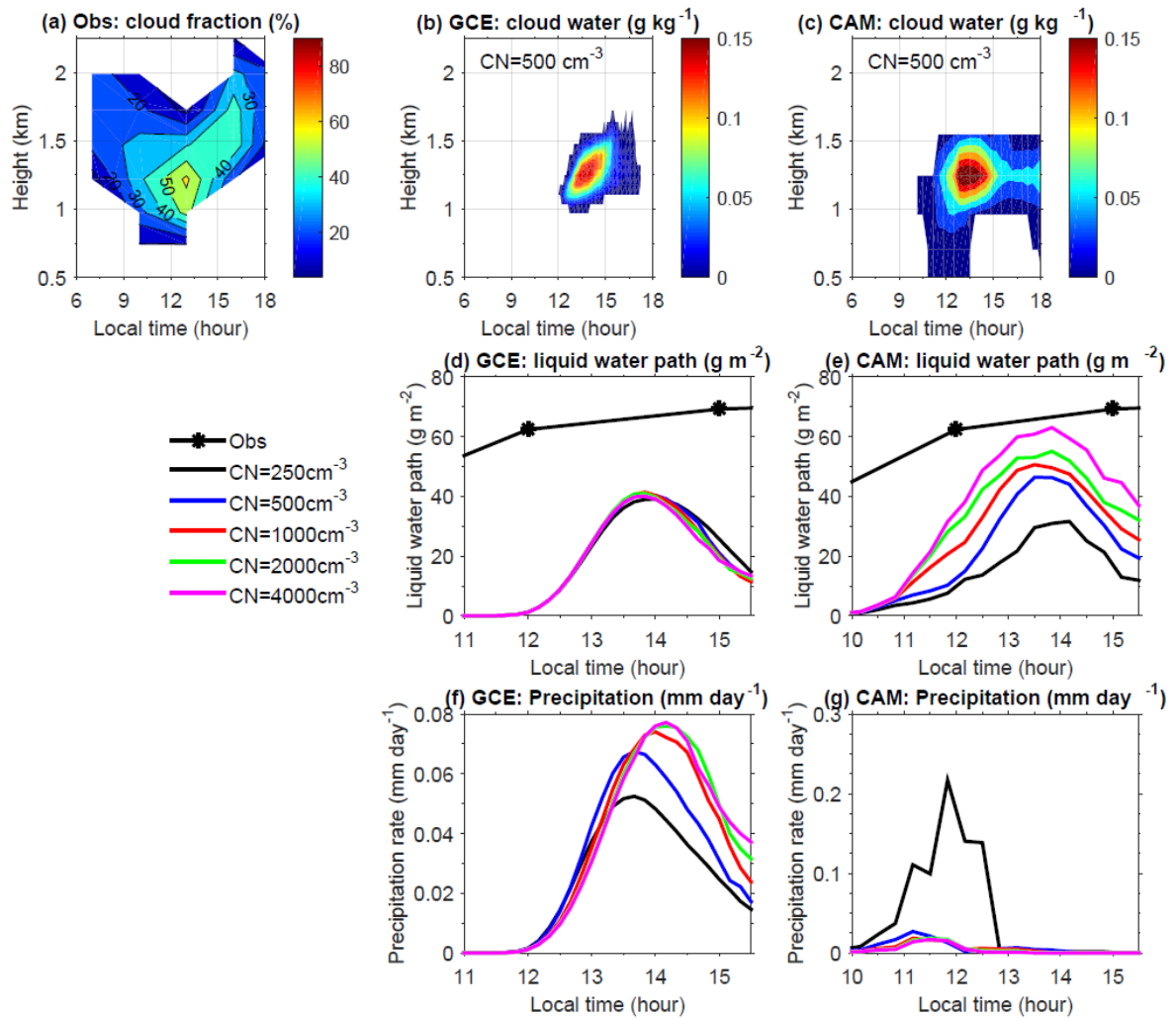
18 Xie, S., Zhang, Y., Giangrande, S. E. , Jensen, M. P., McCoy, R. and Zhang, M.: Interactions  
19 between cumulus convection and its environment as revealed by the MC3E sounding  
20 array, *J. Geophys. Res. Atmos.*, 119, 11,784–11,808, doi:10.1002/2014JD022011, 2014.

21 Xu, K.-M., Cederwall, R. T., Donner, L. J., Grabowski, W. W., et al.: An inter-comparison of  
22 cloud-resolving models with the Atmospheric Radiation Measurement summer 1997  
23 IOP data, *Quart. J. Roy. Meteorol. Soc.*, 128, 593-624, 2002.

24 Xue, H., and Feingold, G.: Large-eddy simulations of trade wind cumuli: Investigation of  
25 aerosol indirect effects, *J. Atmos. Sci.*, 63, 1605–1622, doi:10.1175/JAS3706.1, 2006.

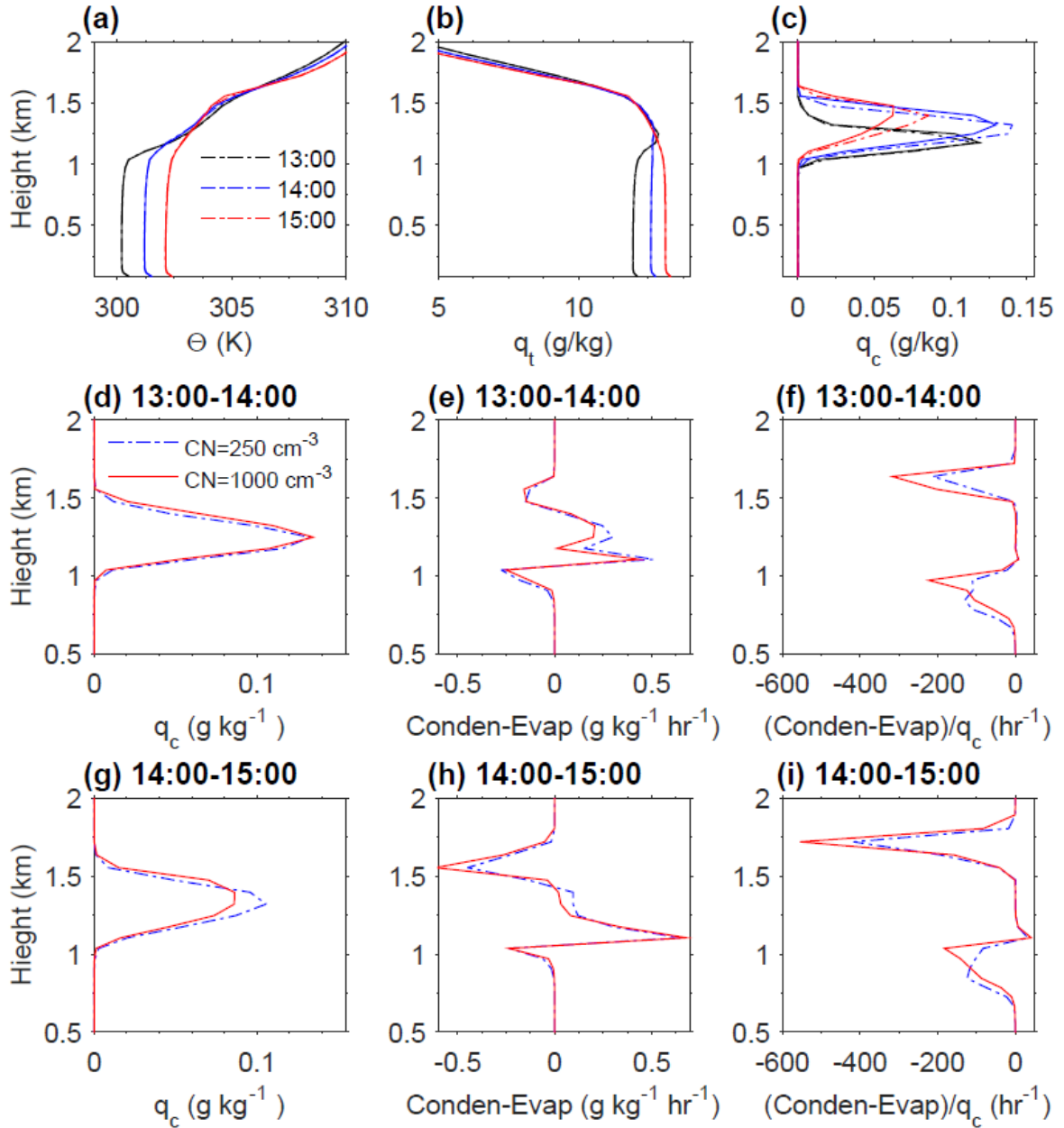
26



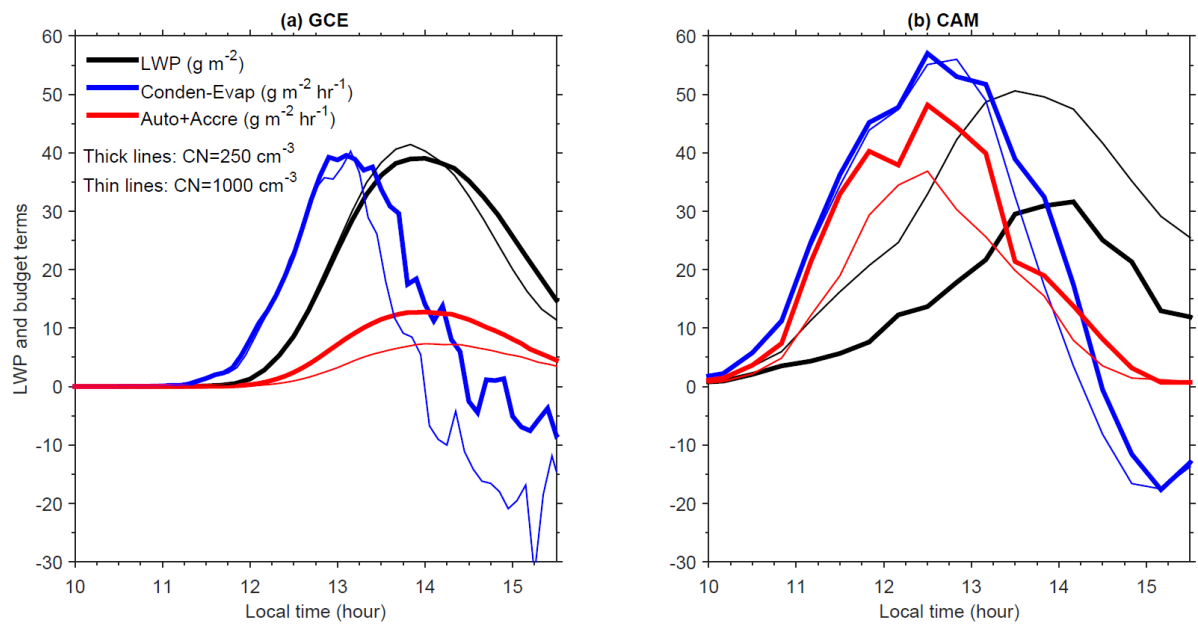


1

2 **Figure 1.** Observed cloud fractions on May 27<sup>th</sup>, 2011 at the SGP site (a); domain  
 3 averaged cloud water content from the GCE model (b) and the single column version of  
 4 CAM (c) for the case assuming a surface aerosol number of  $500 \text{ cm}^{-3}$ ; liquid water path  
 5 and surface precipitation rates from GCE (d, f) and CAM (e, g) with varying surface  
 6 aerosol number concentrations.

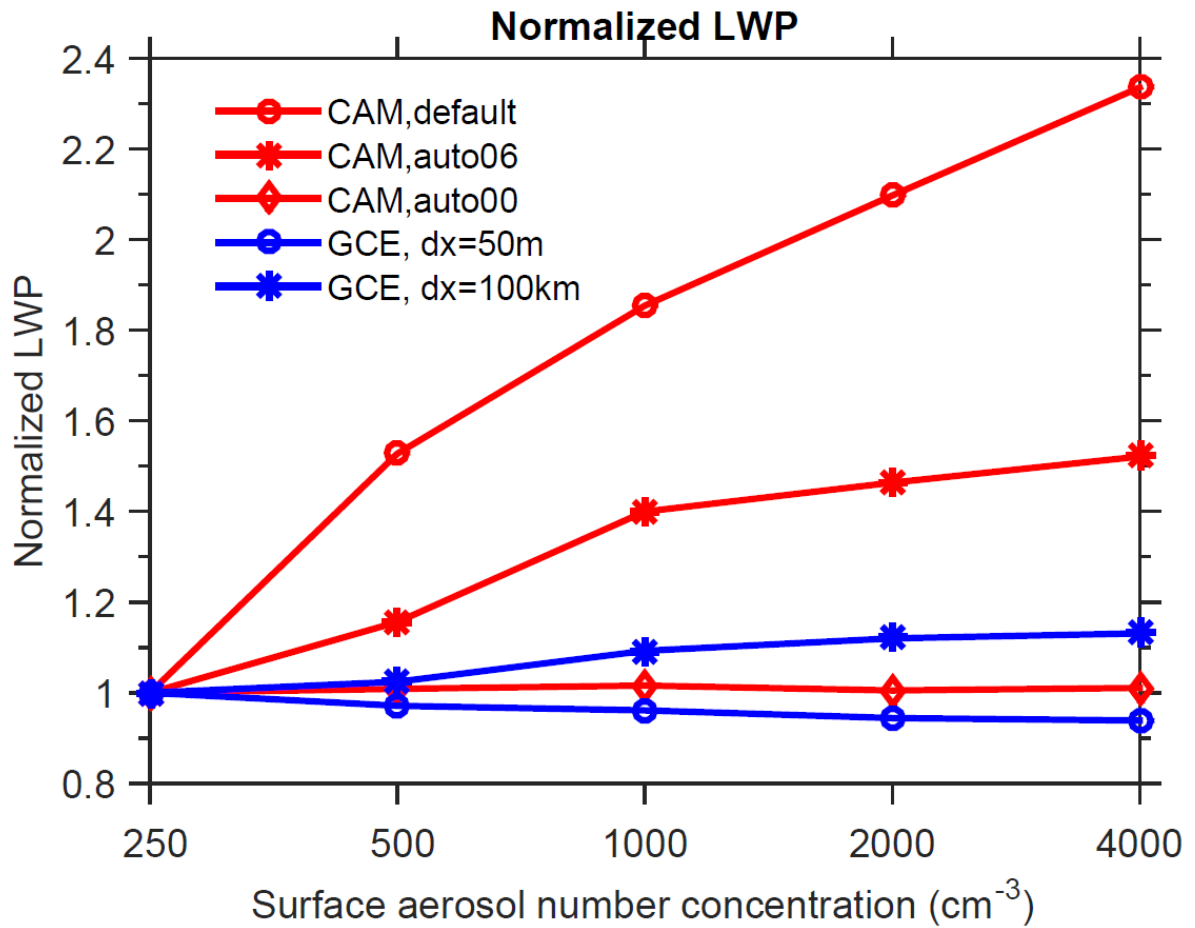


1  
2 **Figure 2.** (a-c) Domain averaged potential temperatures ( $\theta$ ), total water specific humidity  
3 ( $q_t$ ) and cloud water content ( $q_c$ ) at three times (13:00, 14:00 and 15:00) from two GCE  
4 cases with surface aerosol numbers equal to  $250 \text{ cm}^{-3}$  (dash-dotted curves) and  $1000 \text{ cm}^{-3}$   
5 (solid curves). (d-f) Averaged profiles of  $q_c$ , net results of condensation and evaporation  
6 (Condensation-Evaporation), and (Condensation-Evaporation)/  $q_c$  for the 1-hour interval from 13:00 to 14:00  
7 from the two CRM cases with surface aerosol numbers equal to  $250 \text{ cm}^{-3}$  (blue dash-dotted  
8 curves) and  $1000 \text{ cm}^{-3}$  (solid red curves). (g-i) Same as (d-f) except for the 1-hour interval  
9 from 14:00 to 15:00.



1  
2  
3  
4  
5  
6

**Figure 3.** LWP and the column integrated LWP source and sink terms from the case with surface aerosol number concentration equal to  $250 \text{ cm}^{-3}$  (thick lines) and  $1000 \text{ cm}^{-3}$  (thin lines) for (a) GCE and (b) CAM.



1  
2  
3  
4  
5  
6  
7  
8

**Figure 4.** Normalized LWP as a function of surface aerosol concentration in CAM (red curves) and GCE (blue curves). A case for CAM using an autoconversion rate proportional to  $N_d^{-0.6}$  (CAM, auto06) as well as a case in which autoconversion is independent of  $N_d$  (CAM, auto00) is shown. The GCE model was run with a horizontal grid resolution of 50 m (default case) and 100 km.